Spectral nudging to eliminate the effects of domain position and geometry in regional climate model simulations

Gonzalo Miguez-Macho, Georgiy L. Stenchikov, and Alan Robock
Department of Environmental Sciences, Rutgers University, New Brunswick, New Jersey, USA

Received 28 December 2003; revised 20 February 2004; accepted 12 March 2004; published 2 July 2004.

[1] It is well known that regional climate simulations are sensitive to the size and position of the domain chosen for calculations. Here we study the physical mechanisms of this sensitivity. We conducted simulations with the Regional Atmospheric Modeling System (RAMS) for June 2000 over North America at 50 km horizontal resolution using a 7500 km $\times$ 5400 km grid and NCEP/NCAR reanalysis as boundary conditions. The position of the domain was displaced in several directions, always maintaining the U.S. in the interior, out of the buffer zone along the lateral boundaries. Circulation biases developed a large scale structure, organized by the Rocky Mountains, resulting from a systematic shifting of the synoptic wave trains that crossed the domain. The distortion of the large-scale circulation was produced by interaction of the modeled flow with the lateral boundaries of the nested domain and varied when the position of the grid was altered. This changed the large-scale environment among the different simulations and translated into diverse conditions for the development of the mesoscale processes that produce most of precipitation for the Great Plains in the summer season. As a consequence, precipitation results varied, sometimes greatly, among the experiments with the different grid positions. To eliminate the dependence of results on the position of the domain, we used spectral nudging of waves longer than 2500 km above the boundary layer. Moisture was not nudged at any level. This constrained the synoptic scales to follow reanalysis while allowing the model to develop the small-scale dynamics responsible for the rainfall. Nudging of the large scales successfully eliminated the variation of precipitation results when the grid was moved. We suggest that this technique is necessary for all downscaling studies with regional models with domain sizes of a few thousand kilometers and larger embedded in global models. *INDEX TERMS:* 3337 Meteorology and Atmospheric Dynamics: Numerical modeling and data assimilation; 3329 Meteorology and Atmospheric Dynamics: Mesoscale meteorology; 3354 Meteorology and Atmospheric Dynamics: Precipitation (1854); 3319 Meteorology and Atmospheric Dynamics: General circulation; 1620 Global Change: Climate dynamics (3309); *KEYWORDS:* spectral nudging, regional models, downscaling

Citation: Miguez-Macho, G., G. L. Stenchikov, and A. Robock (2004), Spectral nudging to eliminate the effects of domain position and geometry in regional climate model simulations, *J. Geophys. Res.*, *109*, D13104, doi:10.1029/2003JD004495.

1. Introduction

[2] One popular approach to produce high-resolution numerical simulations over a region of interest is to nest a regional model within a coarser global model. This procedure is used routinely for short to medium range numerical weather prediction, and is the subject of multiple studies in the literature. When the nested model technique is employed for climate research it is referred to as dynamical downscaling, and this application is relatively recent [*Dickinson et al.*, 1989; *Giorgi*, 1990]. The use of the nested model technique for climate studies is motivated by the large uncertainties at regional scales of climate simulations produced by general circulation models (GCMs), currently still run at relatively coarse resolution ($\sim$250 km). The uncertainty in climate change scenarios at local scales is a major difficulty for the assessment of impacts of climate change on society. Regional climate simulations with high resolution could also be obtained with variable resolution global models [*Fox-Rabinovitz et al.*, 2000], or by rotating the pole to the area of interest [*Wang et al.*, 1999], but the regional model approach is more accessible to most research groups and computationally cost effective.

[3] At short time ranges, a high-resolution regional model produces better weather forecasts than those of the GCM in which it is nested because it better resolves surface heterogeneity, topography and small scale features in the flow, including growing instabilities. However, the advantage of the nested model diminishes very rapidly, and beyond about 36 h, its skill is no longer higher than that of the GCM [*White et al.*, 1999]. The performance is superior to the GCM's as long as the forecast is mostly an initial value problem for the regional model, but it deteriorates rapidly as

0148-0227/04/2003JD004495

time progresses and the solution turns more into a boundary value problem. The reason for this is that the lateral boundary conditions for the nested model are mathematically not well posed [*Staniforth*, 1997; *Warner et al.*, 1997].

[4] For simulations that span a longer period of time (i.e., running the model in climate mode), the assumption is that the inflow of correct information through the boundaries eventually flushes out errors and the model can still produce meaningful climate statistics. Nevertheless, the behavior of a regional model in climate mode is the subject of active research and controversy (see, for example, *Giorgi and Mearns* [1999] for an overview of issues related to regional climate modeling). Regional models that show good skill for short and medium range forecasts often produce poor climate simulations [e.g., *Takle et al.*, 1999]. Moreover, the reliability of the results, especially its sensitivity, is questionable when, for example, changing the size or the position of the domain sometimes alters results significantly, even at points that stay distant from the boundaries in all cases [*Seth and Giorgi*, 1998]. This indicates that these mixed results may not always be directly due to deficiencies in the model physics or initial state specification, in particular for soil variables.

[5] One factor contributing to the sensitivity to the geometry and position of the domain is that the quality of the boundary data is not homogeneous, and when the boundaries are moved to be over an area where the driving data contain inaccuracies, the poor boundary conditions can contaminate the regional model solution [*Liang et al.*, 2001]. Another factor is that the model physics may be deficient for certain atmospheric situations for which the parameterizations do not work properly. If the domain is moved or expanded to include regions where those situations are more frequent, the errors generated can be advected to the rest of the domain. A more plausible explanation, however, is that the incompatibilities between the model solution and the boundary conditions, already evident in the first days of the simulation, produce an interaction between the model dynamics and the lateral boundaries that affects the solution throughout the domain. The main effect of the interaction with the boundaries is the alteration of the large scales of the circulation. This problem is a consequence of the overspecification of boundary conditions for the atmospheric equations that are solved in the grid [*Staniforth*, 1997]. Lateral boundary conditions are usually imposed following the method of *Davies* [1976], where the model variables are relaxed newtonially to the driving fields in a buffer zone several points wide along the borders of the grid. This relaxation effectively damps small-scale discrepancies that accumulate in the vicinity of the outflow boundaries. However, it does not handle larger scales correctly, and the long waves reflect and interfere within the domain, distorting the circulation.

[6] *Vukicevic and Errico* [1990], in a predictability study with a limited area model, showed that most of the error growth in the regional model occurred in wavelengths longer than 2000 km, whereas errors with smaller scales were damped. The boundary conditions effectively constrain the scales responsible for the error growth only when the domain size is relatively small, of the scale of the minimum wavelength with significant error growth (about 2000 km). In a ''perfect model'' approach, where the boundary conditions for the nested domain are generated by the same model integrated over a much larger area, *de Elía et al.* [2002] found however that the fastest relative error growth occurs at the short scales, which indicates that ideally the boundary conditions do constrain the error growth of the large scales (as compared to the error growth of the short scales), at least for time ranges of a few days.

[7] In reality, either ''perfect'' boundary conditions are used (e.g., reanalysis fields) to drive imperfect regional models, or regional models (more or less ''perfect'') are driven with imperfect boundary conditions from a GCM. In any case, the atmospheric circulation goes through ''media'' of different properties (from the outside to the regional model grid and out of it again), and this makes the boundary interactions (with refractions and reflections of waves) unavoidable. The intensity of the effect may vary with the relative importance of the internal forcings in the nested model or with the strength of the flow entering the boundaries. It may also depend on the ''quality'' of the nested model and the GCM that supplies the driving fields, or to be more specific, on the differences between both.

[8] For longer time simulations with a domain over the Arctic, *Rinke and Dethloff* [2000] also found that most of the contribution to the error in the regional model is from deviations in the large scales. In climate studies over Europe, *Jones et al.* [1995] indicated that the synoptic scales are significantly modified in relatively large domains. These authors identify a domain with dimensions of about 5000 km where the synoptic scale divergence is tolerable, even though not eliminated. A domain of the small size required to constraint the scales for which error growth occurs in a limited area model ($\sim$2000 km) was found to produce very different sensitivities from those of larger domains, which are believed to be more realistic and agree more with sensitivity results from global models [*Seth and Giorgi*, 1998].

[9] As one would expect, the errors in the synoptic circulation translate into errors in all other variables, especially precipitation. *Miguez-Macho et al.* [2004] found that when setting up a regional model for climate applications over North America, the error in the location of the main precipitation pattern was largely due to a systematic distortion of the large-scale flow by the interaction with the lateral boundaries, and not to physical parameterizations or the initialization of soil moisture. They suggested that the large-scale perturbations are preferably organized in patterns dependent on the domain geometry, as well as on the topography in the interior of the grid.

[10] Here we investigated further how the model geometry and position affect the model internal dynamics. We experimented with several positions of the grid, with and without altering its geometry, and results confirmed findings of earlier studies, showing dramatic variations in precipitation amounts and pattern for certain domain position changes. The model biases in all cases organized in a long wave pattern that clearly implicated interaction with the lateral boundaries, since the long waves ''feel'' the lateral boundaries at any point in the interior of the domain.

[11] The distortion of the long wave dynamics limits the downscaling applicability of the nesting technique, because the small-scale variability that the model is supposed to generate from the large scales is therefore also erroneous.

As a solution we propose here the relaxation of the long waves in the domain to those of the driving fields with a spectral nudging technique [*Waldron et al.*, 1996; *von Storch et al.*, 2000; *Miguez-Macho et al.*, 2004]. We conducted the same experiments with nudging of the longest waves in the domain, and the dependence on geometry and size is virtually eliminated.

[12] Nudging only the long waves allows the model to freely develop small-scale variability, and this maintains the utility of the nested model technique as a climate downscaling tool. As a drawback, the effect of small scales on the large-scale flow is greatly diminished, as the large scales are constantly relaxed toward the external fields. This does not represent a serious limitation, because the large scales are provided by the boundary conditions, and the regional model is not meant to modify them significantly. In the last part of the study we assess the effect of the procedure on small scale features, by contrasting the spectral nudging technique with conventional nudging methods in the interior of the domain that damp the short scales already not present in the driving fields.

[13] The paper is organized as follows: Section 2 describes the model and the setup used for the experiments. Section 3 presents results for the experiments for different variations of the domain, and analyzes biases. Section 4 briefly discusses the spectral nudging procedure and shows results for the same experiments as in section 3 but with the nudging of the large scales activated. Section 5 examines the small-scale variability created by the model with spectral nudging of the long waves, and compares results to conventional nudging techniques in the interior of the domain. Section 6 summarizes results and presents conclusions.

2. Model and Experimental Setup

[14] We use the Regional Atmospheric Modeling System (RAMS) version 4.3 [*Pielke et al.*, 1992, *Cotton et al.*, 2003], based on compressible nonhydrostatic hydrodynamic equations and state-of-the art turbulence closure. The model modifications and set up that we implement for the experiments are described in more depth by *Miguez-Macho et al.* [2004]. The main physics options that we chose are a Kain-Fritsch convective scheme [*Kain and Fritsch*, 1990, 1993] with modifications; a ''dumpbucket'' stratiform precipitation scheme as for ClimRAMS [*Liston and Pielke*, 2001]; no explicit microphysics, with cloud water diagnosed; *Mellor and Yamada* [1974] subgrid turbulence; and the two-stream delta-Eddington radiative transfer scheme of *Harrington* [1997]. LEAF2 [*Walko et al.*, 2000], the soil model of RAMS, is run with 11 layers to a depth of 2.5 m.

[15] The horizontal grid uses a rotated polar-stereographic projection and here we utilize a spacing of 50 km. In the vertical, RAMS employs a σ_z terrain-following coordinate system [*Gal-Chen and Somerville*, 1975], and for our experiments the spacing is variable, with 30 vertical levels to a height of approximately 20 km. The minimum vertical resolution is 100 m and the maximum is 1200 m. The smallest grid spacing of 100 m is above the surface, and then the vertical resolution progressively degrades to 1200 m in the upper troposphere and stratosphere. Ten vertical levels are within the boundary layer.

[16] Initial and boundary conditions for the atmospheric fields, as well as initial soil moisture and temperature are from NCEP/NCAR reanalysis [*Kalnay et al.*, 1996]. Sea surface temperatures (SSTs) for most of the Atlantic are 4 km resolution multichannel Advanced Very High Resolution Radiometer satellite retrievals [*Bernstein*, 1982] from the Marine Remote Sensing Laboratory of the Rutgers Institute for Marine and Coastal Sciences, in 3-day composites. For the Pacific, SSTs are weekly averages at 1° latitude-longitude resolution from *Reynolds et al.* [2002].

[17] Boundary conditions are applied following the method of *Davies* [1976] in a 15-point thick buffer zone. The relaxing coefficient follows a parabolic function and is constant in height, as it is standard in RAMS.

[18] The integration time is one month and our region of interest is the U.S. The period chosen for the simulations is June 2000, a month characterized by frequent wave activity in the circulation over North America that resulted in large precipitation amounts over the Great Plains. The control experiment has the grid shown in Figure 1. It comprises most of North America and adjacent ocean areas, including the Gulf of Mexico. The buffer zone along the boundaries is located mostly over ocean points to avoid vertical interpolation problems due to the differences in topography between the reanalysis model and RAMS. The model with the configuration outlined in this section has been thoroughly validated for this grid and period of time in a previous study [*Miguez-Macho et al.*, 2004].

3. Experiments With Different Positions of the Grid

[19] We conduct several experiments to investigate the influence of the position of the domain in the results. Here we focus mainly on precipitation, which is the most difficult variable to simulate and the one that usually shows a large sensitivity to changes in the dynamics. The center of the grid of the control experiment (Figure 1) was successively moved 17° to the west, 10° to the east, 7° to the north, and 10° to the south. The distance moved in each direction is the maximum permitted so that, without changing the grid geometry, the U.S. is contained in the interior of the domain and the buffer zones in the boundaries lie as much over the ocean as they did for the control experiment. In another experiment the grid was rotated so that the long axis of its rectangular shape adopts a North-South orientation. In this case, the number of points was kept at 108 × 150, and the U.S. is also contained in the interior of the domain, out of the buffer zones. The geometry of the grid was only altered in one experiment where it was made a square with 108 × 108 points. The exact position of the different domains is shown together with results from the control experiment in the Figure 2. Because RAMS uses a rotated polar-stereographic projection and we display all results in the same lat-lon projection, grids displaced to the north appear to extend through a much larger region than they actually do. All grids cover exactly the same surface area, except for the experiment with a square domain.

[20] Figure 2 shows precipitation totals for June 2000 for observations and the different grid locations. It is clearly apparent that when displacing the grid, model results vary largely, not only in precipitation amounts but also in pattern.

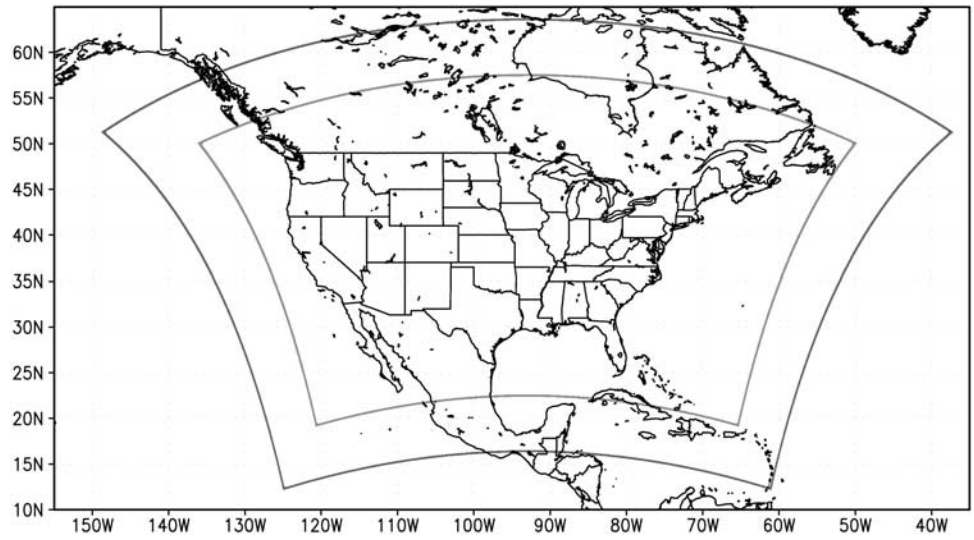

Figure 1. Domain utilized in the control experiment, with an outline of the extent of the buffer zone along the boundaries. See color version of this figure and access the enhanced image in the HTML.

Simulated rainfall totals are also rather different from the observations (Figure 2a), which have a maximum of rainfall approximately on the Oklahoma-Louisiana border with values of 11 mm/day and values of about 7–8 mm/day in a band that stretches in a south to north-northeast direction from northern Texas to the Great Lakes. Precipitation is less in the rest of the US. Only the simulation with the rotated grid (Figure 2g) seems to capture the rainfall pattern in a band structure along the western Plains, but in this simulation precipitation amounts are much reduced as compared to the observations and the other experiments. The rest of the experiments show a band oriented from west to east across the central U.S., except when the grid is displaced to the west or to the north. All simulations, except the one with the rotated grid (Figure 2g), present one clear maximum of rainfall in the vicinity of the Oklahoma-Louisiana border, as in the observations. The experiment with the grid moved to the north shows considerably higher amounts of precipitation than the other ones, extending throughout the southern states of the U.S. with values of 9–10 mm/day.

[21] The observed rainfall pattern for June 2000 (Figure 2a) is typical for wet summers over the Great Plains. An important factor for summer precipitation over this region is the southerly low-level jet on the eastern side of the Rockies, which transports moisture from the Gulf of Mexico. *Byerle and Paegle* [2003] show a strong correlation between the strength of the low-level jet and summer precipitation in the northern Great Plains. They also link persistent anomalous strong zonal flow over the central Rockies with a stronger low-level jet, which results in flooding conditions on the mid and upper Mississippi river basin. The interaction of the large-scale flow with the mountain chain is, for these authors, a scale transfer mechanism between the large-scale flow and regional responses, represented by the low-level jet. Next, we examine the upper level flow for June 2000 and the model bias for each experiment, as examine the relationship of the observed rainfall differences among the experiments with circulation anomalies.

[22] Figure 3 shows monthly mean 200 mb zonal wind from NCEP/NCAR reanalysis; and the 200 mb zonal wind bias for the experiments. The observations indicate a jet at about 45°–50°N with peak values of about 35 m/s across North America and a displacement to the south as the air flow crosses the barrier of the Rockies. A less intense jet stream is also apparent at 20°–25°N centered at 45°W. The biases for all the different experiments show a wave pattern organized by the Rocky Mountains, with maxima and minima along the east side of the mountain chain. When the grid extends sufficiently downstream over the Atlantic Ocean (e.g., Figure 3d), new maxima and minima arise next to the outflow boundary, and these are more intense. Significantly stronger error values appear on the experiment with the grid displaced to the south (Figure 3f). The grid for this experiment has its northern boundary just north of the jet axis, and the sharp temperature gradients that define the tropopause height variation associated with the jet core are not well captured. The jet in this experiment is weaker, and that affects the upper tropospheric circulation everywhere in the grid, overwhelming the wave distribution pattern along the mountains that is observed in all other experiments.

[23] The meridional flow biases also organize in a long wave pattern as indicated in Figure 4. The phase of the waves is not always the same, even though they seem to be organized by the Rocky Mountains with a minimum to the east and a maximum to the west of the cordillera. This is not the case for the experiment with the rotated grid (Figure 4g) and when the grid is displaced to the south (Figure 4f).

[24] Only one of the cases (northern boundary just north of the jet axis, Figure 3f) presents evidence that the wrong position of the grid boundary has a large impact on the upper troposphere wind errors. The other experiments confirm results from a previous study [*Miguez-Macho et al.*, 2004] and indicate that the interaction with the boundaries, and therefore the domain geometry, largely determine the bias patterns in the circulation. Small-scale errors generated inside the model domain eventually grow and affect the synoptic and larger scales. This creates an incompatibility with the

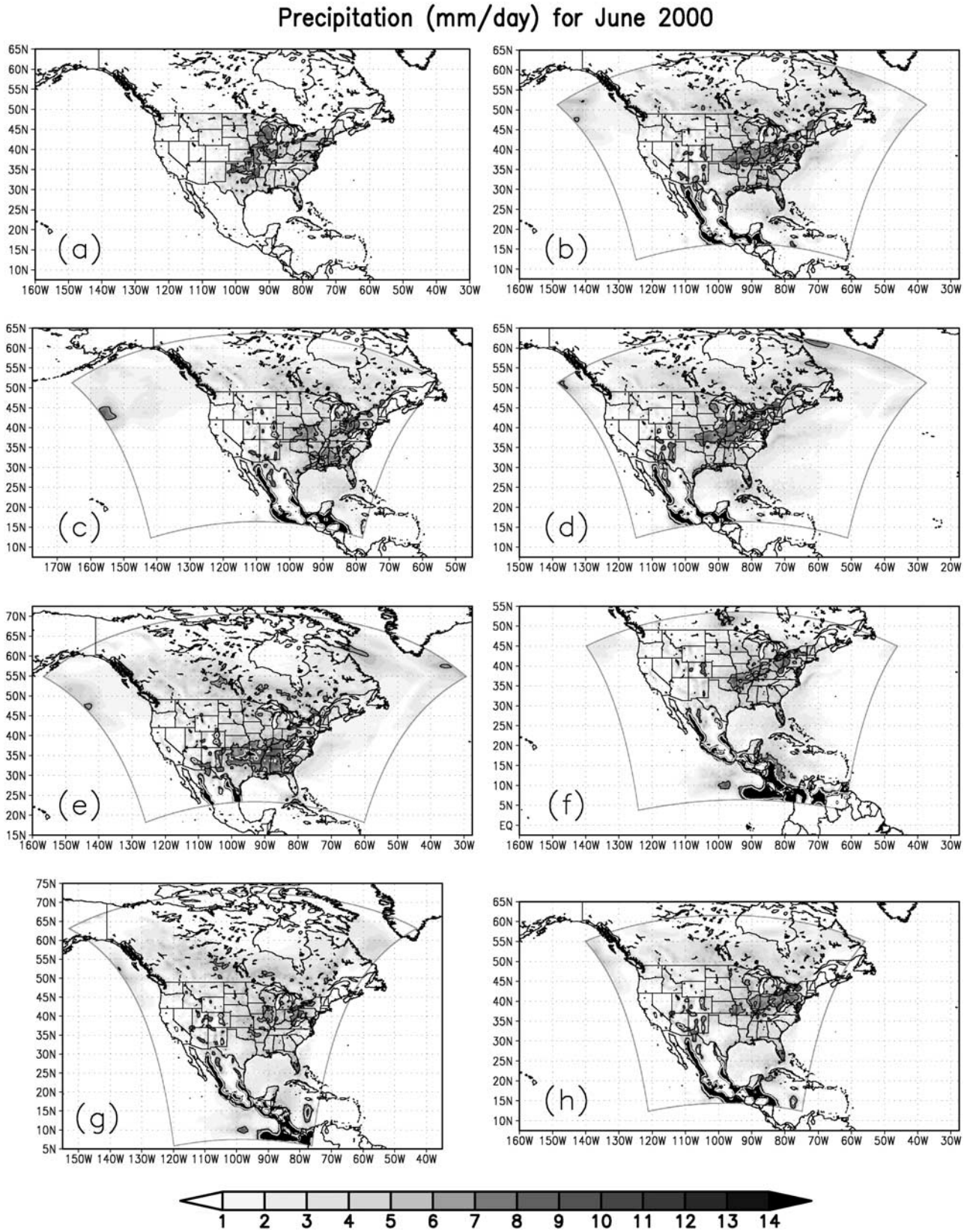

Figure 2. Total precipitation (mm/day) in June 2000 for (a) observed data gridded over the U.S. [*Higgins et al.*, 2000]; (b) RAMS control experiment; experiments with grid displaced (c) to the west; (d) to the east; (e) to the north; (f) to the south; (g) experiment with grid rotated 90°; and (h) experiment with square grid. See color version of this figure and access the enhanced image in the HTML.

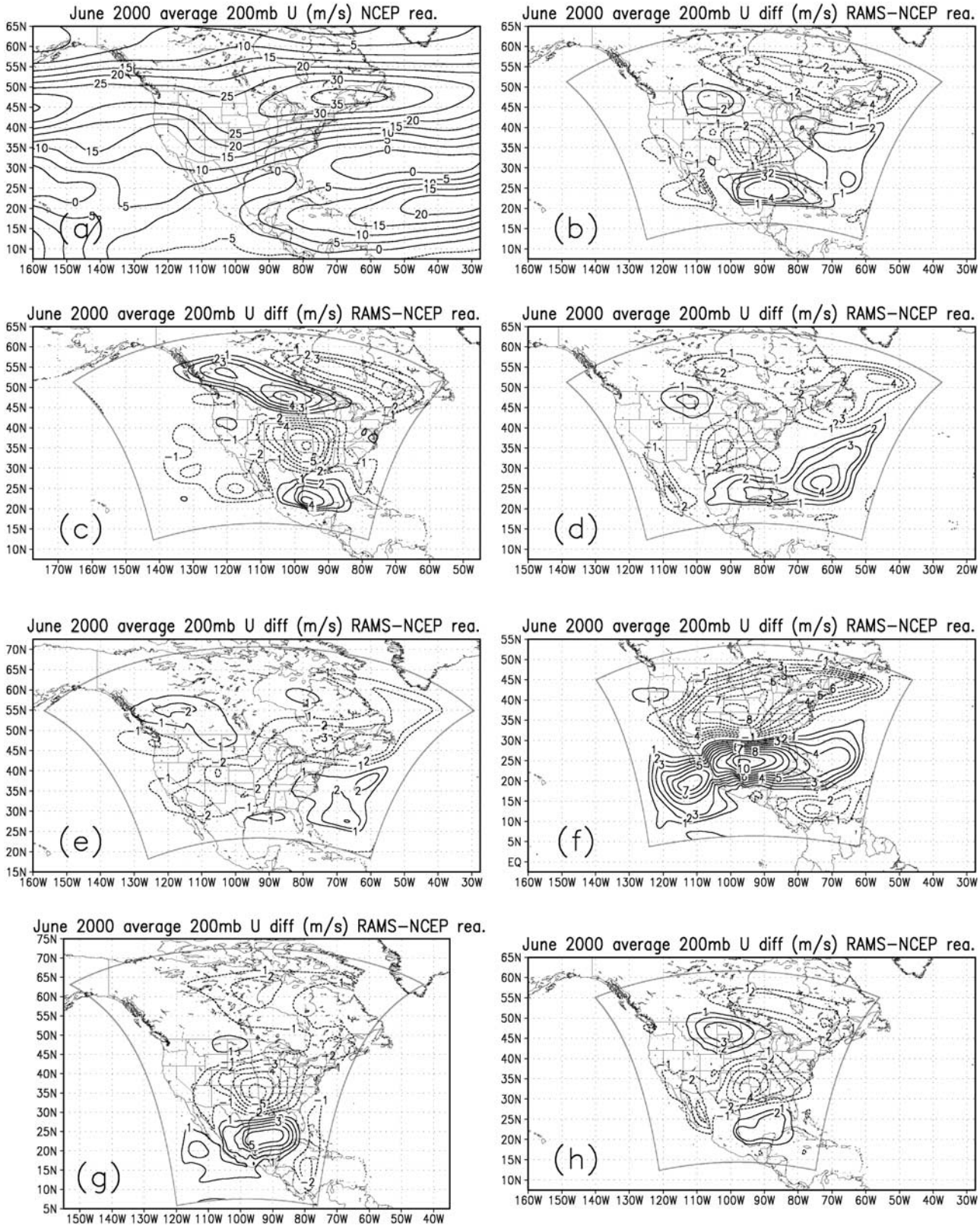

Figure 3. (a) NCEP/NCAR reanalysis average U (m/s) at 200 mb for June of 2000; and 200 mb U biases (m/s) for (b) RAMS control experiment; experiments with grid displaced (c) to the west; (d) to the east; (e) to the north; (f) to the south; (g) experiment with grid rotated 90°; and (h) experiment with square grid. See color version of this figure and access the enhanced image in the HTML.

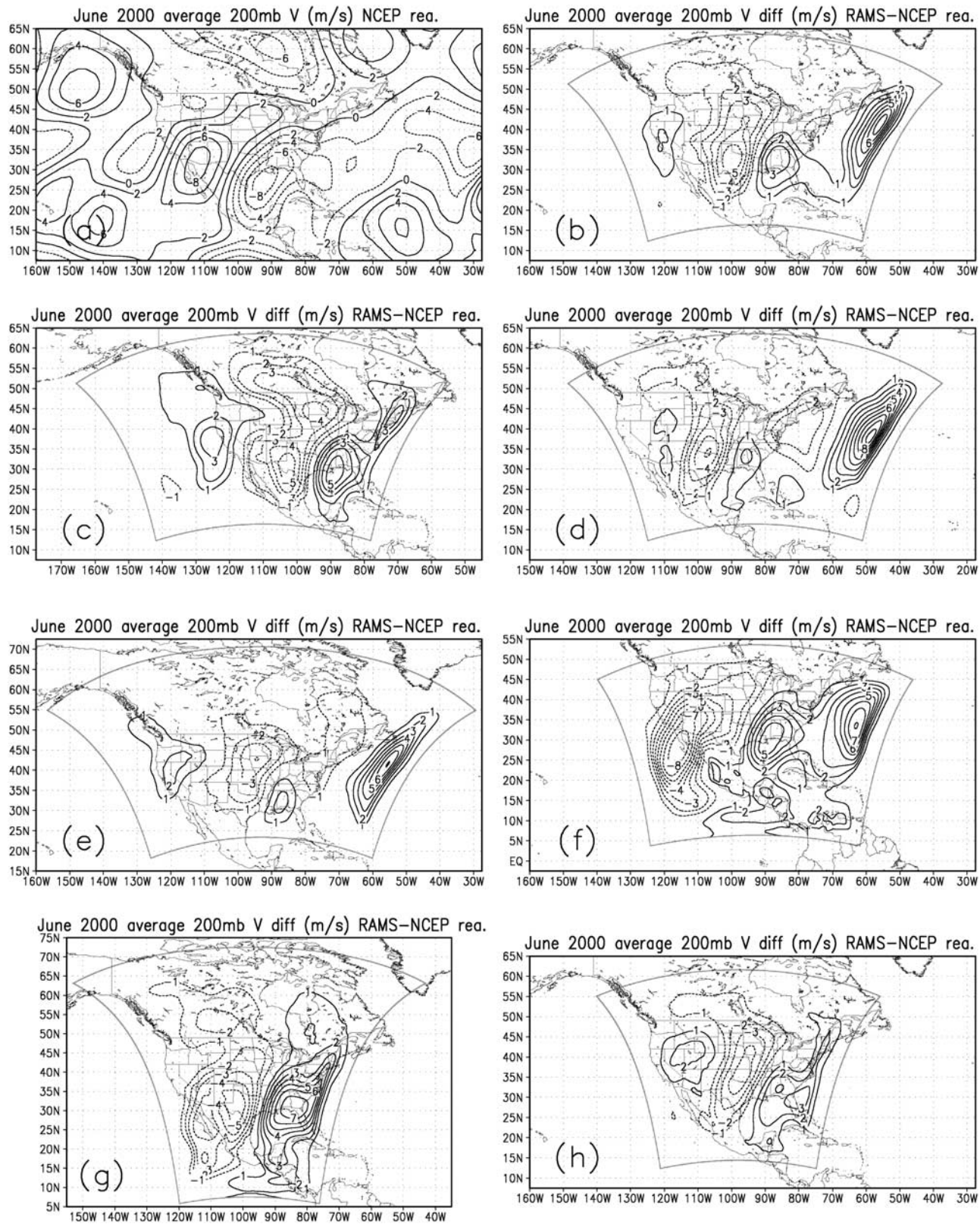

Figure 4. (a) NCEP/NCAR reanalysis average V (m/s) at 200 mb for June of 2000; and 200 mb V biases (m/s) for (b) RAMS control experiment; experiments with grid displaced (c) to the west; (d) to the east; (e) to the north; (f) to the south; (g) experiment with grid rotated 90°; and (h) experiment with square grid. See color version of this figure and access the enhanced image in the HTML.

boundary conditions (there is no feedback permitted, since the boundary data are predetermined) that is more intense in the outflow boundary, where boundary conditions are overspecified. The large scale waves from the model reflect from the boundary and interfere inside the domain; the result is the longwave pattern that we see in the upper air wind biases in Figures 3 and 4, which correspond to shifts in the successive synoptic wave characteristic of the period. The intensity of the biases varies largely with the domain position, even when the model physics are exactly the same in all experiments, and the areas covered are not so drastically different from each other (North America and the surrounding oceans). The alterations in the circulation translate into the rather different precipitation patterns that are shown in Figure 2.

[25] *Jones et al.* [1995] and earlier predictability studies with limited area models [*Vukicevic and Errico*, 1990] suggest that reducing the domain size is the only manner to avoid physical inconsistencies between the regional model solution and the driving fields. However, if the area of interest is North America and one wants to keep the boundaries and buffer zones over ocean areas, it is not possible to reduce the domain size much more than, for example, that of the square grid that we chose for one of our experiments. In this case, the synoptic scales of the flow were also different from reanalysis.

4. Experiments With Spectral Nudging

[26] *Miguez-Macho et al.* [2004] proposed a spectral nudging technique to solve the problem of the distortion of the large scale dynamics by interaction with the boundaries, and therefore allow the use of relatively large domains for dynamical downscaling applications. Spectral nudging was originally introduced for a regional model by *Waldron et al.* [1996] and has also been applied for climate simulations by *von Storch et al.* [2000]. It consists of adding a new term to the tendencies of the variables that relaxes the selected part of the spectrum to the corresponding waves from reanalysis,

$$\frac{dQ}{dt} = L(Q) - \sum_{|n|\le N} \sum_{|m|\le M} K_{mn} \cdot (Q_{mn} - Q_{o\,mn}) e^{ik_m x} e^{ik_n y}. \qquad (1)$$

Q is any of the prognostic variables to be nudged, L is the model operator, and Q_o is the variable from the driving fields. Q_{mn} and Q_{omn} are the spectral coefficients of Q and Q_o respectively. K_{mn} is the nudging coefficient, which can vary with m and n and also with height; m and n are the wave numbers in the x and y directions in polar stereographic projection that roughly correspond to the east-west and north-south directions, respectively. The wave vector components k_m and k_n in the x and y directions depend on the domain size D_x and D_y in the corresponding direction and wave number,

$$k_m = \frac{2\pi \cdot m}{D_x}; \qquad k_n = \frac{2\pi \cdot n}{D_y}. \qquad (2)$$

[27] The spectral decomposition is performed on the difference fields $Q - Q_o$, which are quasiperiodic, since they are always close to zero along the boundaries. The relaxation term, with only the coefficients for the selected part of the spectrum, is transformed from wave space to physical space and added to the tendency for the prognosed variable Q. Because of the orthogonality of the functions of the Fourier expansion, only the same part of the spectrum of variable Q will be affected by the relaxation.

[28] The variables nudged are u, v, θ_{il} and π' (winds, modified equivalent potential temperature that is conserved in both ice-to-liquid and liquid-to-vapor phase transformations, and perturbation Exner function). We choose not to nudge moisture fields because their variations in the horizontal, and especially in the vertical, can be very pronounced and likely to be missed by coarse resolution reanalyses. The strength of the nudging depends on coefficient K_{mn}, which is set to be a function of height, being zero in the boundary layer and increasing smoothly from about 1500 m above the terrain to become constant in the upper troposphere with a characteristic time for the relaxation of 5000 s. The variables in the boundary layer are not nudged because the coupling of the atmosphere and land surface is strongest there. The reanalysis fields were generated with a coarser model (T62) with a topography that can be quite different from the one in our experiments, and therefore by making K_{mn} zero in the lowest 1500 m above the terrain we allow the model to develop a boundary layer totally compatible with its orography and land cover.

[29] In the experiments where the grid is rectangular with 150 $\times$ 108 points, nudging is applied for wave numbers 0, 1, 2 and 3 in the x direction and 0, 1 and 2 in the y direction. This is the equivalent of setting $M = 3$ and $N = 2$ in (1). When the grid is rotated 90° the wave numbers nudged for each dimension are reversed, and when the grid is a square with 108 $\times$ 108 points only wave numbers 0, 1 and 2 are nudged for both x and y direction. For all experiments, the nudged wave numbers correspond to wavelengths of about 2500 km and longer (wave number 3 and smaller in the grid dimension with 7500 km, and about wave number 2 and smaller in the one with 5400 km). The minimum wavelength nudged of 2500 km corresponds approximately to the wave structure of the error patterns shown in Figure 3 and 4. Moreover, waves of about that length and larger were identified by *Vukicevic and Errico* [1990] as the scales having most error growth in limited area models.

[30] Figure 5 shows precipitation results for the monthly simulations with similar domains and set up as in Figure 2, but with nudging of the large scales applied as previously described. Precipitation patterns and amounts are very similar now in all experiments and the spurious variations due to displacements of the domain or changes in geometry are eliminated. These coincident results occur even though the boundary layer variables, as well as moisture at all levels, are not nudged. Precipitation totals show reduced amounts in the Northern Great Plains (compare with observations in Figure 5a), but this negative result is on the other hand positive if it is taken as an indication that the model, with all its problems in physical parameterizations, is still free to develop small scales at which most of the precipitation processes take place.

5. Effects of Small-Scale Variability

[31] In this section we assess the behavior of the model at small scales when we relax the synoptic scales to reanalysis.

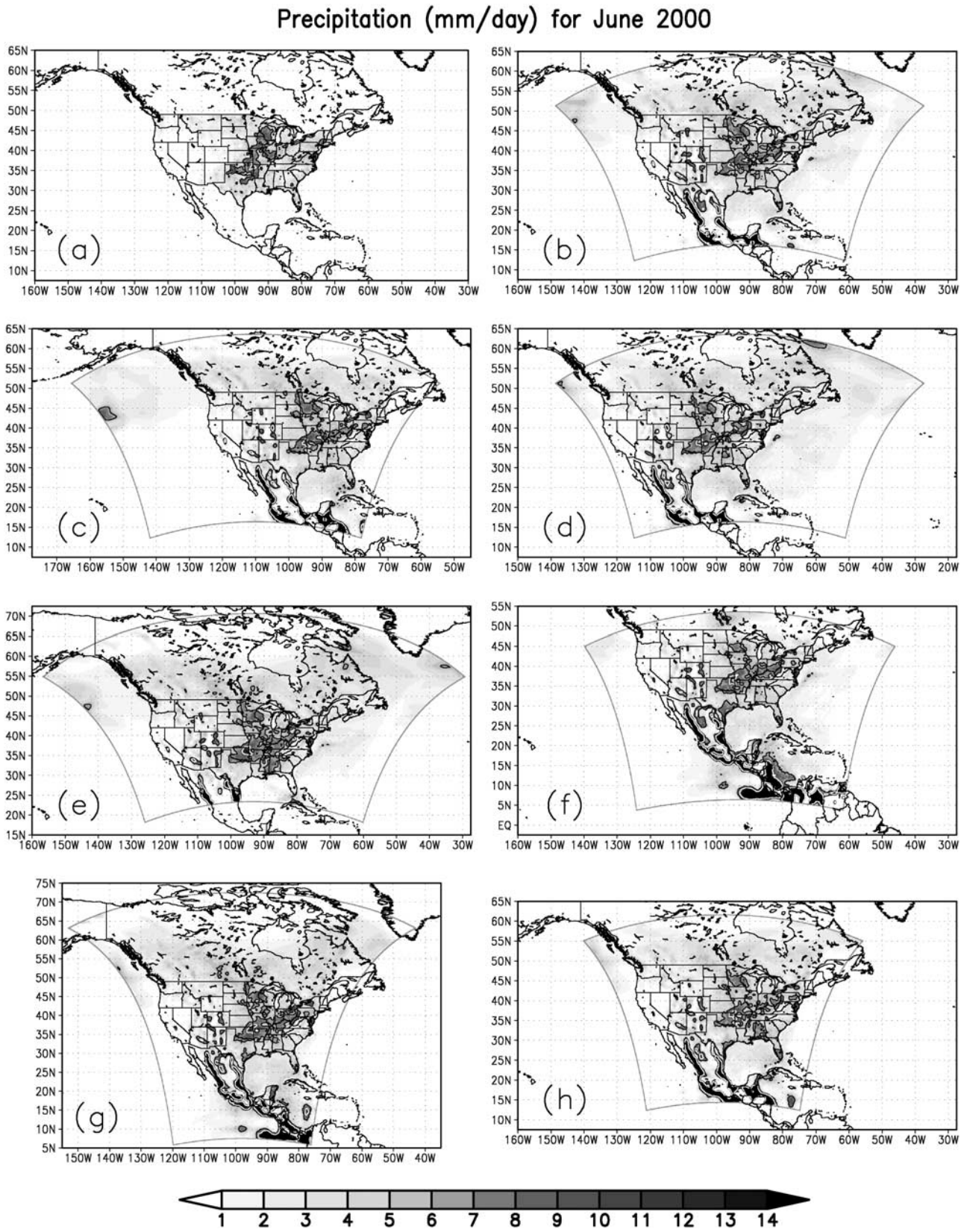

Figure 5. Total precipitation (mm/day) in June 2000 for (a) observed data gridded over the U.S. [*Higgins et al.*, 2000]; RAMS simulations with spectral nudging for (b) control experiment; experiments with grid displaced (c) to the west; (d) to the east; (e) to the north; (f) to the south; (g) experiment with grid rotated 90°; and (h) experiment with square grid. See color version of this figure at back of this issue, and access the enhanced image in the HTML.

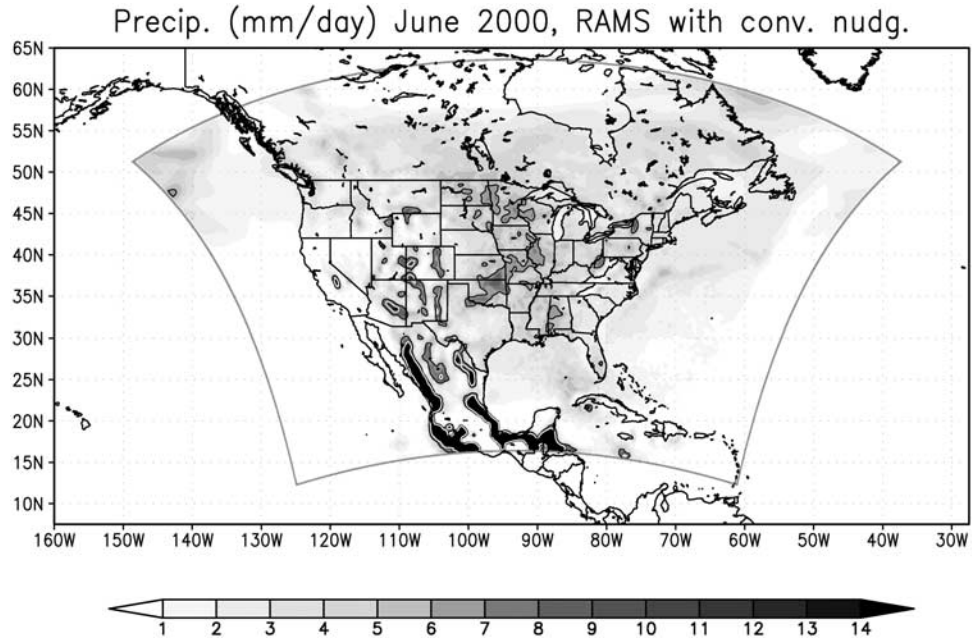

Figure 6. Total precipitation (mm/day) for June 2000 for RAMS experiment with the grid in the control position and conventional nudging applied in the interior of the domain. See color version of this figure and access the enhanced image in the HTML.

For comparison, we conduct a new simulation with the grid in the control position and all wavelengths of u, v, θ_{il} and π' nudged to reanalysis above the boundary layer throughout the domain with a characteristic time of 5000 s (same as in the spectral nudging experiments). This is conventional Newtonian relaxation (as applied in the boundaries) to reanalysis of those variables and levels.

[32] Figure 6 shows precipitation results for this experiment with conventional nudging in the interior of the grid. Compared to Figure 5b, results for the simulation with identical domain and settings, but with nudging of the long waves in the grid, precipitation is sensibly reduced when conventional relaxation is used. Differences in other variables between both simulations are on average not very large and look rather noisy and unorganized (not shown). However, it is precisely that small-scale variability that causes the large differences in rainfall produced between both simulations.

[33] To quantify the effect of nudging on different scales, we perform a spectral analysis of the kinetic energy following the method of *Errico* [1985] for a rectangular domain. For analysis purposes, the kinetic energy of waves with the module of the two-dimensional wave vector

$$k - \frac{1}{2}\Delta k < \left(p^2 + q^2\right)^{1/2} < k + \frac{1}{2}\Delta k; \tag{3}$$

belonging to the interval

$$k_l - \frac{1}{2}\Delta k < \left(k_m^2 + k_n^2\right)^{1/2} < k_l + \frac{1}{2}\Delta k; \tag{4}$$

was calculated and attributed to a one-dimensional wave vector k_l. Here Δk is the minimum wave vector for a given domain and resolution,

$$\Delta k = \frac{2\pi}{\Delta s}\frac{1}{(L-1)}; \tag{5}$$

with Δs the grid spacing (same in y and x directions for all cases), and L the maximum of L_x and L_y, the dimensions of the grid in x and y directions respectively. Therefore

$$k_l = l\Delta k; \qquad l = 0, 1, \cdots, (L-1)/2 \tag{6}$$

where l is a generalized wave number that characterizes waves moving in all directions but with the wave vectors from interval (4).

[34] Figure 7 depicts the time evolution of the $\log_{10}$ of the amplitude of the kinetic energy spectral coefficients at 500 mb as a function of l. At the initial time, kinetic energy in all three simulations shows a sharp decrease in amplitude for wave numbers larger than 7 (equivalent to wavelengths of about 1000 km), which is the minimum contained in the reanalysis fields used to initialize the model and thereafter as boundary conditions. The model employed in the reanalysis project is a T62 spectral model, but the fields that we use here were archived on a 2.5° × 2.5° grid after being filtered and smoothed to a resolution of T36, equivalent to minimum wavelengths of 10°, or about 1,000 km. The simulation with conventional nudging has about the same small amplitude beyond that wave number 7 for the rest of the month (Figure 7c). However, the experiment with spectral nudging of the long waves rapidly develops small scales (Figure 7b) (after only 6 h, not shown), and at day 10 the fields have the same amplitude in large wave numbers as when there is no nudging at all in the interior of the domain (Figure 7a). Figure 7 is for 500 mb, but the structure is similar at all other levels, except at those that lie in the boundary layer, where no nudging of any kind is applied in any of the three simulations.

[35] Figure 8 shows the vertical structure of the differences between the spectral amplitudes of the kinetic energy of the control experiment, with no nudging of

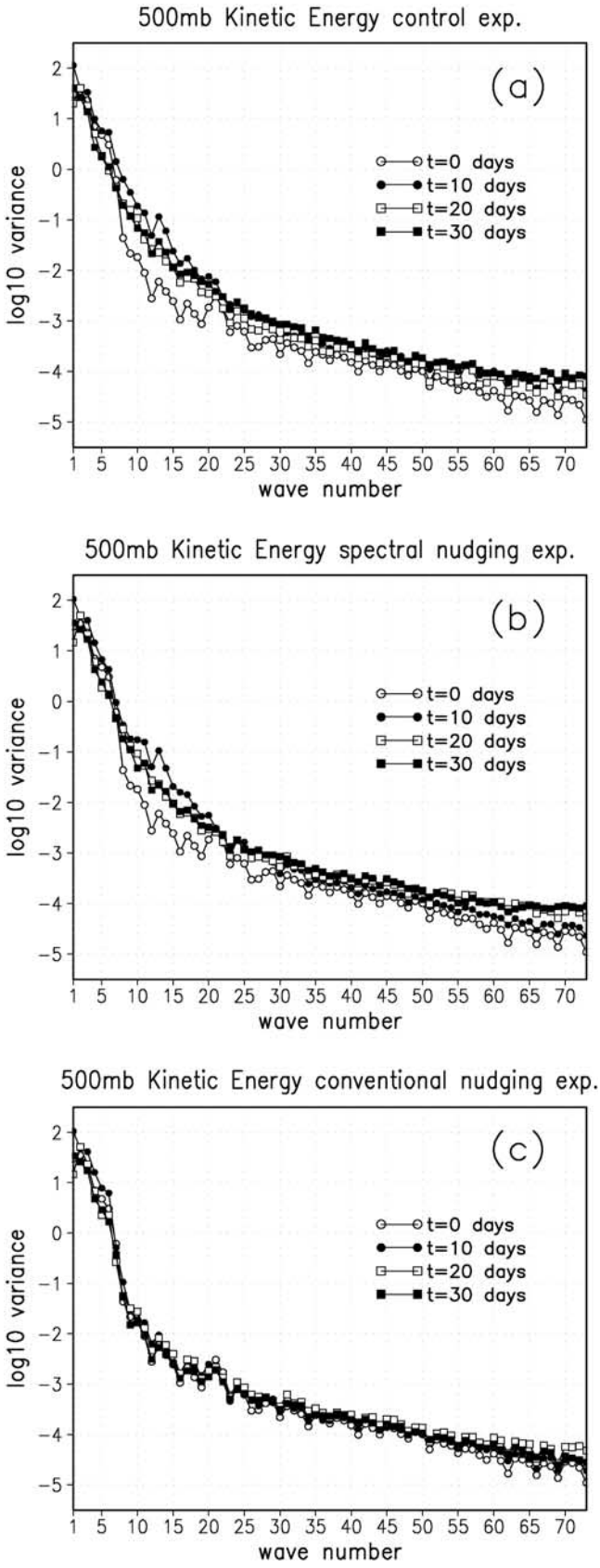

any kind, and the spectral nudging experiment, and those of the simulation with conventional nudging in the interior of the grid. Results are normalized by the amplitudes of the coefficients of the experiment with conventional nudging, so that for example a value of 1 for a particular l and level indicates similar amplitude as in conventional nudging; a value of 2 corresponds to twice the energy for that particular scale, and so on. As already shown for 500 mb in Figure 7, nudging only the large scales (Figure 8b) maintains at all levels the small scale variability developed by the model when no nudging is applied (Figure 8a). The energy at small scales in the experiment with spectral nudging of the long waves and the simulation with no nudging is several times larger than the present in the experiment with conventional nudging, which dumps scales beyond the resolution of reanalysis ($l > 7$). At wave numbers less than 7, the three simulations have similar energy amplitude. The same is true below 850 mb, since no relaxation of any kind is applied there (the nudging coefficient is zero in the lowest 1500 m above the terrain).

[36] The experiment with nudging of the long waves and the conventional nudging experiment are very similar in terms of biases in wind and other variables (not shown), since most of their amplitudes are contained in the large scales (especially for mass fields such as temperature and geopotential heights) and these are relaxed to reanalysis in both cases. Figures 7 and 8 show that the difference between those experiments is in the amplitude of the small scales above the boundary layer. The much higher precipitation totals over the Great Plains obtained with the experiments with spectral nudging of the large scales as compared to when using conventional nudging; is therefore explained by the presence of the small-scale variability in the mid and upper troposphere that the model with nudging of the large scales develops.

6. Summary and Conclusions

[37] In this study we investigated the dependence of results on the position and size of the model's grid when using a regional model for dynamic downscaling. We find that the large scale circulation is distorted by the interaction of the flow with the lateral border of the grid, where boundary conditions are imposed on the atmospheric variables by a relaxation of the model solution to reanalysis fields.

[38] Small-scale errors throughout the domain eventually grow and affect the synoptic scales of the model's solution, diverting it from observations. This creates physical incompatibilities between the model's fields and reanalysis at the outflow boundaries, where boundary conditions are actually

Figure 7. Spectrum of the kinetic energy at 500 mb. The x axis corresponds to l, the index of the two-dimensional wave number and the y axis to $\log_{10}$ of the variance. (a) Control simulation, where there is no nudging at all in the interior of the grid; (b) experiment with spectral nudging; and (c) experiment with conventional nudging in the interior of the domain. Curves are for initial time (open circles), day 10 (closed circles), day 20 (open squares) and day 30 (closed squares). See color version of this figure and access the enhanced image in the HTML.

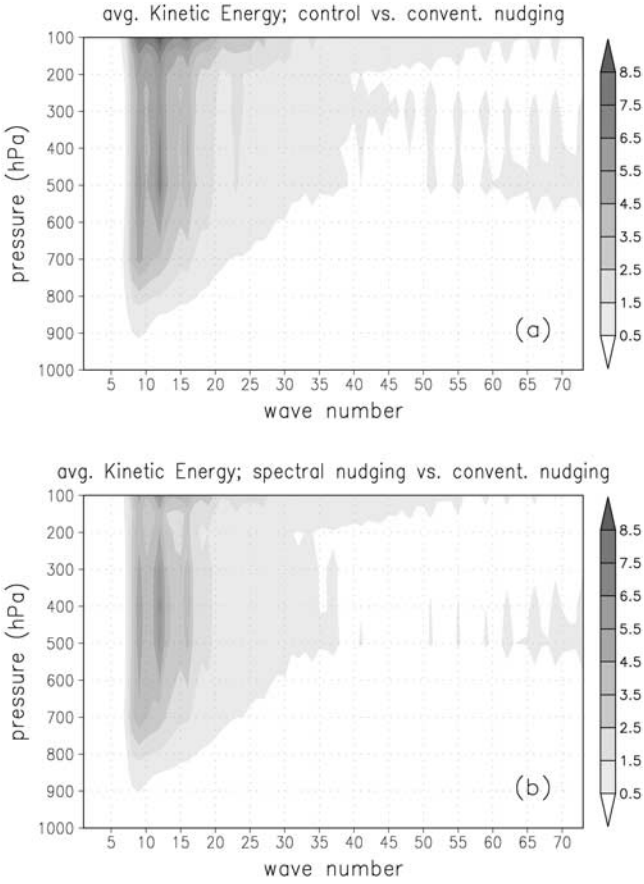

Figure 8. Vertical structure of the differences, averaged for the whole month of integration, between the spectral amplitudes of the kinetic energy of (a) the control experiment, with no nudging of any kind, and (b) the spectral nudging experiment; and those of the simulation with conventional nudging in the interior of the grid. Results are normalized by the amplitudes of the coefficients of the experiment with conventional nudging. See color version of this figure and access the enhanced image in the HTML.

overspecified [*Staniforth*, 1997]. The Davies boundary conditions damp relatively small-scale disturbances smoothing the fields near the lateral boundaries. However, they are unable to handle long waves that reflect from the sponge layer along the boundaries. These reflecting waves interfere and distort the synoptic circulation across the grid, overwhelming the supply of correct information entering through the inflow boundaries. The resulting biases in the circulation show longwave patterns, displaced and organized by topographic features in the domain (in our case, the Rocky Mountains), whose interaction with the flow plays an important role in the amplification and creation of synoptic waves in the dynamics.

[39] These results confirm those from a previous study by *Miguez-Macho et al.* [2004] for a domain over North America. *Rinke and Dethloff* [2000] also found that most of the errors in climate simulations with a regional model over the Arctic came from differences in wavelengths longer than 1000 km. The impossibility of avoiding distortion in the synoptic scales for sufficiently large domains has also been suggested in earlier studies with regional models applied for climate downscaling over Europe [*Jones et al.*, 1995] and for predictability [*Vukicevic and Errico*, 1990].

[40] The month simulated here was June of 2000, where abundant precipitation fell on the Great Plains. Most of the summer rainfall in this region is convective in nature, and related to mesoscale dynamics such as elongated squall lines and mesoscale convective systems. The moisture necessary to produce large precipitation totals is fed from the Gulf of Mexico by the Great Plains low-level jet, also a mesoscale feature. These small-scale processes responsible for most of the rainfall occur well in the interior of the domains that we chose for all experiments. However, they are not independent from the large-scale environment. Stronger low-level jets have been correlated with intense upper level zonal flow over the Rockies [*Byerle and Paegle*, 2003], and mesoscale convective complexes are favored by a strong low-level jet and weaker upper tropospheric inertial stability [*Pan et al.*, 2000].

[41] In our experiments, distortion of the large-scale flow varies depending on the position of the domain boundaries. This results in different conditions for the development of the mesoscale dynamics responsible for rainfall, and as a consequence in different precipitation results, both in amount and in pattern. Dependence of precipitation amounts on domain geometry in regional climate simulations has been previously reported in the literature [*Seth and Giorgi*, 1998; *Liang et al.*, 2001].

[42] As a solution for the problem of the dependence of results on the grid's size and position, which is intrinsic to the nesting procedure, we tested the spectral nudging technique [*Waldron et al.*, 1996; *von Storch et al.*, 2000]. *Miguez-Macho et al.* [2004] employed nudging of waves 2500 km and longer in a previous study and showed that it corrected the distortion of the large scales and improved results largely. The relaxation was not applied at any level for specific humidity, and for any variable in the boundary layer. Here we followed a similar procedure and demonstrated that with nudging of the large scales the model results no longer depended on the position and size of the grid.

[43] To study the behavior of the model when we utilize spectral nudging, we compared results of the experiment where we nudge the large scales to those of a simulation where conventional relaxation (all spectrum is nudged, instead of only the long waves) was applied with the same timescale and for the same variables and levels as in spectral nudging. Precipitation was significantly reduced when conventional nudging was used. Both experiments had small biases in the mid and upper air fields, which indicates that the synoptic scales closely followed the observations. Spectral analysis showed that both experiments had similar amplitude of small-scale variability in the lower atmosphere, since no relaxation was applied there. The main difference appeared in the mid and upper troposphere, where the experiment with spectral nudging of the long waves had several times more energy in scales below the resolution of the reanalysis fields than the conventional nudging experiment. The relaxation to reanalysis at all scales damped the energy that the model developed at wavelengths smaller than the ones already

present in the reanalysis. Spectral nudging of the long waves maintained that energy with amplitudes similar to those found when no nudging of any kind is applied in the interior of the domain.

[44] Dynamic fluctuations with scales smaller than about 2500 km in the mid and upper troposphere (and not in the boundary layer) were responsible for the larger precipitation in the experiment with spectral nudging than in the experiment with conventional nudging, and the higher rainfall amounts were closer to observed rain gauge data for the period. The small-scale responses to the large-scale environment were successfully developed by the model when spectrally nudged in the long waves, and these were especially important in the mid and upper atmosphere. Spectral nudging, even when applied only to a large-scale component of the atmospheric flow, allows the accurate development of small-scale processes, like convective precipitation. Parameterizations of such processes still have to be improved in the models, but our approach eliminates the dependence on the domain choice that complicates the interpretation of the responses of the model to changes in the physics.

[45] The experiments here were performed for a summer month, when the internal forcings in the model, especially convection, are relatively strong with respect to the lateral boundary forcings. For a winter situation, when the circulation is stronger and the control of the lateral boundary conditions over the model internal dynamics is more pronounced, it is possible that the distortion of the synoptic scales and the dependence of results on the position of the grid may have different intensity than in this study for June of 2000 over North America. We do expect, however, that in a winter case the large scales will also be altered by interaction with the imposed lateral boundary conditions to a certain degree.

[46] These results suggest that for all downscaling experiments with regional models with domains of the order of a few thousands kilometers or larger, spectral nudging of the long waves is necessary for accurate simulation of small scale circulation and to eliminate spurious influence of the boundaries on large scale circulation inside the domain. Only after this problem is addressed, can the relative effects of local surface interactions and large scale forcing be studied, and the small scale, regional patterns of climate change be accurately simulated.

[47] **Acknowledgments.** We thank Chris Weaver, Jan Paegle, Bob Walko, and two reviewers for valuable comments on the work, and Chris Castro and A. Beltran for the Kain-Fritsch scheme. NCEP Reanalysis data and Reynolds SST data were provided by the NOAA-CIRES Climate Diagnostics Center, Boulder, Colorado, at http://www.cdc.noaa.gov/. Supported by the Center for Environmental Prediction, Cook College, NASA Goddard Institute for Space Sciences grant NCC5-553, and New Jersey Department of Environmental Protection contracts SR-00-048 and SR-02-082.

References

Bernstein, R. L. (1982), Sea surface temperature estimation using the NOAA-6 advanced very high resolution radiometer, *J. Geophys. Res.*, *87*, 9455–9465.

Byerle, L. A., and J. Paegle (2003), Modulation of the Great Plains low-level jet and moisture transports by orography and large-scale circulations, *J. Geophys. Res.*, *108*(D16), 8611, doi:10.1029/2002JD003005.

Cotton, W. R., et al. (2003), RAMS 2001: Current status and future directions, *Meteorol. Atmos. Phys.*, *82*, 5–29.

Davies, H. C. (1976), A lateral boundary formulation for multi-level prediction models, *Q. J. R. Meteorol. Soc.*, *102*, 405–418.

de Elía, R., R. Laprise, and B. Denis (2002), Forecasting skill limits of nested, limited-area models: A perfect-model approach, *Mon. Weather. Rev.*, *130*, 2006–2023.

Dickinson, R. E., R. M. Errico, F. Giorgi, and G. T. Bates (1989), A regional climate model for the western United States, *Clim. Change*, *15*, 383–422.

Errico, R. M. (1985), Spectra computed from a limited area grid, *Mon. Weather. Rev.*, *113*, 1554–1562.

Fox-Rabinovitz, M., G. L. Stenchikov, M. J. Suarez, L. L. Takacs, and R. C. Govindaraju (2000), A uniform-and variable-resolution stretched-grid GCM dynamical core with realistic orography, *Mon. Wea. Rev.*, *128*, 1883–1898.

Gal-Chen, T., and R. C. J. Somerville (1975), On the use of coordinate transformation for the solution of the Navier-Stokes equations, *J. Comput. Phys.*, *17*, 209–228.

Giorgi, F. (1990), On the simulation of regional climate using a limited area model nested in a general circulation model, *J. Clim.*, *3*, 941–963.

Giorgi, F., and L. O. Mearns (1999), Introduction to special section: Regional climate modeling revisited, *J. Geophys. Res.*, *104*(D6), 6335–6352.

Harrington, J. Y. (1997), The effects of radiative and microphysical processes on simulated warm and transition season Arctic stratus, Ph.D. dissertation, 289 pp., Dept. of Atmos. Sci., Colo. State Univ., Fort Collins, Colo.

Higgins, R. W., J. E. Janowiak, and Y.-P. Yao (2000), Improved U.S. precipitation quality control system and analysis, *Clim. Predict. Cent. Atlas 7*, Natl. Cent. for Environ. Predict., Washington, D. C.

Jones, R. G., J. M. Murphy, and M. Noguer (1995), Simulations of climate change over Europe using a nested regional climate model. I: Assessment of control climate, including sensitivity to location of lateral boundaries, *Q. J. R. Meteorol. Soc.*, *121*, 1413–1449.

Kain, J. S., and J. M. Fritsch (1990), A one-dimensional entraining/detraining plume model and its application in convective parameterization, *J. Atmos. Sci.*, *33*, 1890–1910.

Kain, J. S., and J. M. Fritsch (1993), Convective parameterization for mesoscale models: The Kain-Fritsch scheme, in *The Representation of Cumulus Convection in Numerical Models*, *Meteorol. Monogr. Ser.*, vol. 24, pp. 165–170, Am. Meteorol. Soc., Boston, Mass.

Kalnay, E., et al. (1996), The NCEP/NCAR 40-year reanalysis project, *Bull. Am. Meteorol. Soc.*, *77*, 437–471.

Liang, X.-Z., K. E. Kunkel, and A. N. Samel (2001), Development of a regional climate model for U.S. Midwest applications. Part 1: Sensitivity to buffer zone treatment, *J. Clim.*, *14*, 4363–4378.

Liston, G. E., and R. A. Pielke Sr. (2001), A climate version of the regional atmospheric modeling system, *Theor. Appl. Climatol.*, *68*, 155–173.

Mellor, G. L., and T. Yamada (1974), A hierarchy of turbulence closure models for planetary boundary layers, *J. Atmos. Sci.*, *31*, 1791–1806.

Miguez-Macho, G., G. L. Stenchikov, and A. Robock (2004), Regional climate simulations over North America: Interaction of local processes with improved large-scale flow, *J. Clim.*, in press.

Pan, Z., R. W. Arritt, M. Segal, T.-C. Chen, and S.-P. Weng (2000), Effects of quasi-stationary large-scale anomalies on some mesoscale features associated with the 1993 flood: A regional model simulation, *J. Geophys. Res.*, *105*(D24), 29,551–29,564.

Pielke, R. A., et al. (1992), A comprehensive meteorological modeling system-RAMS, *Meteorol. Atmos. Phys.*, *49*, 65–78.

Reynolds, R. W., N. A. Rayner, T. M. Smith, D. C. Stokes, and W. Wang (2002), An improved in situ and satellite SST analysis for climate, *J. Clim.*, *15*, 1609–1625.

Rinke, A., and K. Dethloff (2000), On the sensitivity of a regional Arctic climate model to initial and boundary conditions, *Clim. Res.*, *14*(2), 101–113.

Seth, A., and F. Giorgi (1998), The effects of domain choice on summer precipitation simulation and sensitivity in a regional climate model, *J. Clim.*, *11*, 2698–2712.

Staniforth, A. (1997), Regional modeling: A theoretical discussion, *Meteorol. Atmos. Phys.*, *63*, 15–29.

Takle, E. S., and Coauthors (1999), Project to intercompare regional climate simulations (PIRCS): Description and initial results, *J. Geophys. Res.*, *104*(D16), 19,433–19,461.

von Storch, H., H. Langenberg, and F. Feser (2000), A spectral nudging technique for dynamical downscaling purposes, *Mon. Weather Rev.*, *128*, 3664–3673.

Vukicevic, T., and R. M. Errico (1990), The influence of artificial and physical factors upon predictability estimates using a complex limited-area model, *Mon. Weather Rev.*, *118*, 1460–1482.

Waldron, K. M., J. Paegle, and J. D. Horel (1996), Sensitivity of a spectrally filtered and nudged limited area model to outer model options, *Mon. Weather Rev.*, *124*, 529–547.

Walko, R. L., et al. (2000), Coupled atmospheric-biophysics-hydrology models for environmental modeling, *J. Appl. Meteorol.*, *39*, 931–944.

Wang, M., J. Paegle, and S. DeSordi (1999), Global variable resolution simulations of Mississippi river basin rains of summer 1993, *J. Geophys. Res.*, *104*(D16), 19,399–19,414.

Warner, T. T., R. A. Paterson, and R. E. Treadon (1997), A tutorial on lateral boundary conditions as a basic and potentially serious limitation to regional numerical weather prediction, *Bull. Am. Meteorol. Soc.*, *78*, 2599–2617.

White, B. G., J. Paegle, W. J. Steenburgh, J. D. Horel, R. T. Swanson, L. K. Cook, D. J. Onton, and J. G. Miles (1999), Short-term forecast validation of six models, *Weather Forecast.*, *14*, 84–107.

G. Miguez-Macho, A. Robock, and G. L. Stenchikov, Department of Environmental Sciences, Rutgers University, 14 College Farm Road, New Brunswick, NJ 08901, USA. (gonzalo@envsci.rutgers.edu; robock@envsci.rutgers.edu; gera@envsci.rutgers.edu)

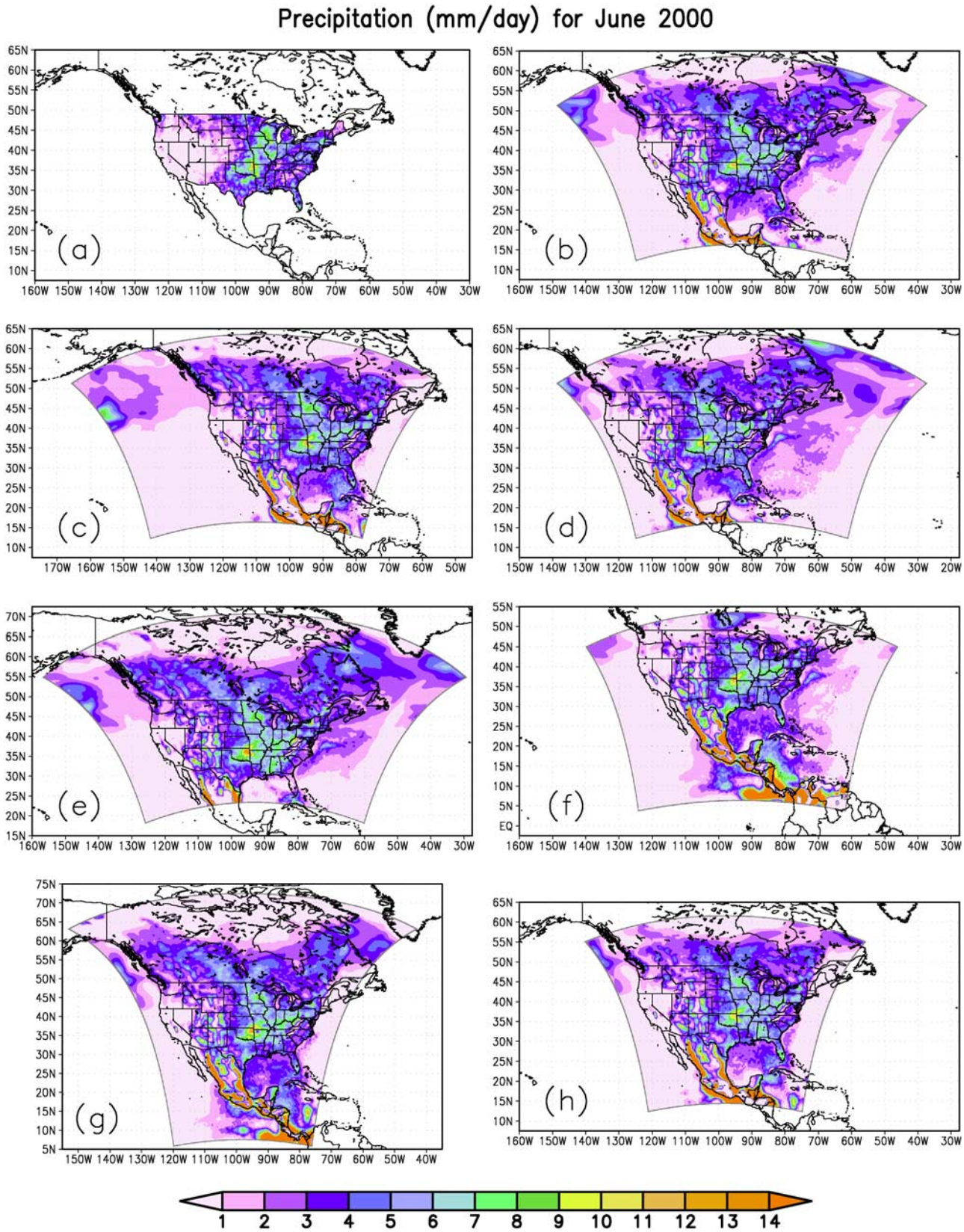

Figure 5. Total precipitation (mm/day) in June 2000 for (a) observed data gridded over the U.S. [*Higgins et al.*, 2000]; RAMS simulations with spectral nudging for (b) control experiment; experiments with grid displaced (c) to the west; (d) to the east; (e) to the north; (f) to the south; (g) experiment with grid rotated 90°; and (h) experiment with square grid.